HHS Public Access

Author manuscript

Ann N Y Acad Sci. Author manuscript; available in PMC 2018 December 01.

Published in final edited form as:

Ann N Y Acad Sci. 2017 December ; 1410(1): 93–106. doi:10.1111/nyas.13572.

Bone quality changes associated with aging and disease: a review

Adele L. Boskey and **Laurianne Imbert**

Hospital for Special Surgery and Weill Cornell Medical College

Abstract

Bone quality encompasses all the characteristics of bone that, in addition to density, contribute to its resistance to fracture. In this review, we consider changes in architecture, porosity and composition, including collagen structure, mineral composition and crystal size. These factors all are known to vary with tissue and animal ages, and health status. Bone morphology and presence of micro-cracks which also contribute to bone quality, will not be discussed in this review. Correlations with mechanical performance for collagen cross-linking, crystallinity and carbonate content are contrasted with mineral content. Age dependent changes in humans and rodents are discussed in terms of using rodent models of disease. Examples are osteoporosis, osteomalacia, osteogenesis imperfecta, and osteopetrosis, in both humans and animal models. Each of these conditions, along with aging, are associated with increased fracture risk for distinct reasons.

Keywords

FTIR imaging; microCT; bone composition; osteoporosis; osteogenesis imperfecta

Measuring bone quality

Bone quality is generally defined as a collection of properties that contribute to fracture risk in addition to bone mineral density (BMD).[1,2,3] This collection of variables, summarized in Figure 1, consists of architecture and geometry, turnover, cortical porosity, damage, and composition (extent of mineralization, mineral stoichiometry, collagen, other matrix constituents, and water content). These measures, in addition to BMD, explain bone strength. Numerous techniques exist to measure these quality variables, reviewed elsewhere, [4] along with a few newer techniques referenced later. Architecture and geometry can be measured by micro-, nano-, or peripheral-computerized tomography and by nuclear magnetic resonance imaging.[5–7] Bone turnover is generally measured by histomorphometry[8] although it can be approximated from urinary turnover-markers.[9] Macroscopic cortical porosity has been measured by microcomputed tomography (micro-CT) and MRI;[10] however, newer methods exist based on Raman spectroscopy[11–13] and short-wave infrared Raman spectroscopy[14] that have also been applied to measure water content. Damage has been assessed by basic Fuschin staining[15] and more recently by synchrotron radiation transmission x-ray microscopy with an x-ray negative stain.[16] Compositional measurements

Contact: Laurianne Imbert imbertL@hss.edu.

include classic methods and newer techniques reviewed elsewhere.[4] NMR was similarly used to measure water content. Backscattered electron imaging and BMDD measurements along with vibrational spectroscopic imaging methods, provide insight into spatially resolved compositional properties. In this review, we focus primarily on spectroscopic techniques, with limited illustrations from other measurements.

The majority of the results presented in this review were produced using spatially-resolved spectroscopic imaging techniques. Readers are referred to several recent reviews[4,17,18,19,20] for discussion of spectroscopic principles, sample preparation methods, data analysis and limitations of these techniques. These techniques vary greatly in resolution; in general, the better the spatial resolution, the worse the signal-to-noise ratio (Table 1).

Several features of bone composition can be derived from these spectroscopic data sets. Because vibrations that are strong in Raman spectra tend to be weaker in Fourier transform infrared spectroscopy (FTIR) and vice versa, these techniques are often viewed as complimentary. Generally, in either technique, complex spectra may be deconvoluted by second derivative spectroscopy (less observer dependent), curve fitting or other deconvolution algorithms, factor analysis and other multidimensional methods (e.g., Principal component analysis). Many bone quality parameters assessed by vibrational spectroscopic imaging have been validated by comparison to independent analytical techniques using purified model compounds. The major variables reported for FTIR Imaging (FTIRI) are mineral-to-matrix ratio (mineral content per organic matrix), carbonate-to-phosphate, also called carbonate-to-mineral ratio (extent of carbonate substitution in the apatite lattice), crystallinity (crystal size and perfection), collagen cross-link ratio (related to enzymatic cross-links) and acid phosphate substitution (inversely related to mineral maturity) (Fig. 2). In addition, aggregates of DNA can be imaged, and sugar and lipid contents can be estimated. In Raman, proteoglycan content and porosity or water content similarly can be estimated. Values for these measurements may be reported in areas between fluorescent labels (to mark newly formed bone), adjacent to specific morphologic domains, in entire trabeculae or cortices, or some combination of these sites. Because the characteristics and kinetics of the bone constituents and their changes with disease differ between the periosteal, osteonal and endosteal compartments of cortical bone, measurements also should report the specific compartment examined[21]. A recent study[22] showed sampling five random sites throughout the human cortex or analyzing the entire section did not affect average values, although the spread of the data (line width at half maximum of the pixel distribution or heterogeneity) was quite different.

Bone quality changes during development

The first study of bone composition based on vibrational spectroscopic imaging used Raman analysis to examine mouse calvaria parietal bone from embryonic day 13.5 (6 days before birth) to 6 months of age.[23] Over this time period, mineral content increased gradually from being undetectable (embryonic day 13.5–14.5) to detectable levels of carbonate-containing hydroxyapatite mineral at embryonic day 15.5. In these mice, mineral-to-matrix ratio increased gradually and continuously until post-natal day 3, again increasing at 6 months,

whereas carbonate-to-phosphate ratio was constant from embryonic day 15.5 to post-natal day 3, then increased gradually.

Using FTIR, microcomputed tomography and mechanical testing, female BALB mouse tibias were evaluated at eight time periods, between 1 and 40 days of age, then compared to tibias of 450-day-old mice.[24] During the first 40 days, bone mineral density increased, as did polar moment of inertia and elastic modulus; however, cortical porosity decreased. In these mice tibias, mineral-to-matrix ratio increased from 12% of the 450-day value at 1 day to 65% of that value by day 30. In contrast, collagen crosslinking decreased from 112% (day 1) to 80% (day 30). in this mouse model, crystallinity remained essentially unchanged. In a similar study, male C57BL/6 mice, with and without exercise, were evaluated with co-localized Raman and nanoindentation using linear regressions and non-linear multidimensional visualization.[25] Based on univariate analysis, material properties of 4- and 5-month-old specimens were not significantly different but for a marginal increase in collagen cross-linking ratio and a marginal decrease in hardness at 4 months. Mineral-to-matrix ratio, carbonate-to-phosphate ratio and crystallinity were significantly greater in 19-month-old (skeletally mature, old) bones compared to the values in skeletally mature young bones (4- and 5-month-old combined). Crosslink ratio and nanoindentation measurements were not significantly different between the two age groups. Exercise had no significant effect on measures by either modality. In linear regressions of single Raman metrics with mechanical properties across all age groups, plasticity index was significantly and positively correlated to both carbonate-to-phosphate and mineral-to-matrix ratios. Bone modulus positively correlated with crystallinity. Bone modulus, hardness and creep viscosity negatively correlated with cross-linking ratio. In the 4–5 month age group, mineral-to-matrix ratio positively contributed to the modulus, while cross-link ratio had a significant negative contribution. Cross-link ratio was the only Raman metric that significantly correlated to hardness (negative effect). Carbonate-to-phosphate ratio positively contributed to plasticity index. In the 19-month-old bones, only mineral-to-matrix ratio contributed to mechanical properties. Unfortunately, similar studies have not been reported in other mouse models, or with other bones, except for those that served as controls for transgenic animals.[25]

In a study[26] examining areas that mineralized over a period of 386 days compared to interstitial areas mineralized over 550 days, fluorochrome-labeled rabbit osteons were reported to rapidly mineralize between days 1 and 18, reaching 67% of interstitial bone levels. This increase was followed by a slower, more progressive accumulation of mineral up to day 350. By day 351, a plateau was reached. Carbonate-to-protein ratio similarly increased rapidly during the first 18 days, reaching 73% of interstitial bone levels and plateauing by 315 days.

Non-human primates, such as baboons, provide insight into Haversian remodeling changes bone tissue with age. In an FTIRI, Raman and mechanical study of baboons from newborn to 32 years of age, [27,28] consistent systematic variations in bone properties were found as a function of tissue age in osteons. The patterns observed were independent of animal age and positively correlated with bone tissue elastic behavior measured by nanoindentation. The mineral-to-matrix ratio was correlated with the animal age in both old (interstitial) and

newly-formed bone tissue; carbonate-to-phosphate ratio and crystallinity increased with animal and osteonal age and porosity, then reached a plateau.

In humans, loss of cancellous bone begins during the third decade of life in both men and women and is accelerated with menopause[29,30] later on, cortical bone loss occurs after menopause or sex steroid-deficiency in aging men and is associated with increased porosity.[31] Age-related changes in human trabecular bone architecture include decreased trabecular numbers, thickness, and connectivity with decreases in thickness being larger in men than in women;[32] women losing most bone by decreases in trabecular number and men by trabecular thinning.[30] While acquiring human biopsies for age-dependent studies is difficult, they are sometimes available as controls from other studies. We have examined iliac crest biopsies from individuals with juvenile osteoporosis[33] and post-menopausal women with fragility fractures.[22,34] The female non-fractured controls from these two studies are shown as a function of age for some of the FTIRI parameters for cortical and cancellous bone in Figure 3A and 3B. Seen here and in general agreement with the findings in other species,[27,28] with increasing chronologic age, mineral-to-matrix ratio, carbonate-to-phosphate ratio and collagen cross-link ratio increased, crystallinity increased and then reached a plateau while acid phosphate substitution decreased. A study comparing newly formed bone in healthy aging and postmenopausal osteoporosis showed that compositional changes depended on subject age, tissue age and health[35]. These results in healthy iliac crest biopsies suggested that the kinetics of maturation could be altered with advancing age. Both subject age and tissue age must be taken into account when examining how diseases affect these parameters.

Bone quality changes in disease

Bone is a heterogeneous tissue that is constantly in flux, reflected by the activities of the three major bone cell types: osteoblast, osteocyte and osteoclast. When the interactions among these cell types are disrupted due to aging, injury and environmental changes, primary and secondary bone diseases may develop. In this review, we will consider a few examples of these diseases to demonstrate the various changes that affect the tissues' mechanical performance.

Osteoporosis

Osteoporosis, associated with an increased risk of non-traumatic (fragility) fractures, occurs in both women and in men. High resolution NMR, for example, detailed differences between male and female osteoporosis[36] with elderly women having lower apparent bone volume fraction (BV/TV) and trabecular thickness (Tb.Th) than elderly men; elderly osteopenic women (based on BMD) had lower BV/TV and Tb.Th than elderly normal women. In a study comparing mechanical strength of biopsies obtained from the femoral neck of hip fracture patients during replacement surgery, ultimate stress of trabecular bone was significantly higher in men than in women.[37] Few studies exist, however, comparing bone quality in men and women with osteoporosis. Existing studies show that vertebral bone samples of men have higher values of BV/TV and Tb.Th compared to women[38] and cortical

porosity measured by high resolution peripheral quantitative CT (HR-pQCT) is higher in radius and tibia of women than in men.[39]

In contrast, there are numerous studies of bone quality in osteoporotic women, many (not included here, but recently reviewed[40]) consider the effects of pharmaceutical interventions on bone quality measurements. Bone mineral density distribution (BMDD) based on calcium levels, is lower in iliac crest biopsies[41] and in vertebral bodies[42]of women with fractures compared to historic controls; tissue from vertebrae with acute compression fractures had a larger variation in matrix mineralization depending on the stage of repair. Similarly, BMDD of cancellous bone in premenopausal women with idiopathic osteoporosis was decreased to lower values than age-matched controls.[43]

In age-matched, fracture-free controls, FTIR microscopy (FTIRM) found the bone in iliac crest biopsies of individuals with fractures had greater crystallinity than in controls.[44] In a study of 54 iliac crest biopsies (32 from individuals with fractures, 22 without) who had significantly different spine but not hip BMDs and ranged in age from 30 to 83 years, using FTIRI, the metrics associated with fracture risk in a linear regression model were increased cortical and cancellous collagen maturity, increased cortical mineral/matrix ratio and cancellous crystallinity.[34] When matched for both BMD and age, a study of 60 pairs of iliac crest biopsies from women with and without fractures found most of these predictors (mineral-to-matrix ratio, collagen maturity, crystallinity) which increase with age were no longer significant, but the carbonate-to-phosphate ratio in both cancellous and cortical bone, and increased heterogeneity of collagen maturity for cancellous bone were significant.[22]

Raman analysis also showed femoral trabecular bone and iliac crest cortical bone in women with fractures had a higher carbonate-to -amide I area ratio and carbonate-to-phosphate ratio, respectively[45]. Mineral-to-matrix ratio (based on Raman) and indentation modulus were reduced in cancellous bone of females with osteoporosis.[46] Collagen pyridinoline content was elevated in osteoporotic cases as was lipid content, most other Raman changes were associated with aging.[35] MicroCT microstructural changes in osteoporotic bone as compared with age-matched controls include decreased bone volume, trabecular number, and connectivity density and increased of trabecular separation[47,48]; however, these changes are dependent on resolution of the image.[49] Increased cortical porosity in osteoporotic tissue is also noted by microCT.[50]

There are fewer studies of quality changes in osteoporotic men, however, an early investigation of 108 men (mean age 52 years) with lumbar osteopenia, based on spinal radiographs found there was at least one vertebral crush fracture in 62 patients, and none in the other. Trabecular separation (Tb.Sp) was increased in the fracture group; whereas trabecular number (Tb.N) decreased.[51] Logistic regression showed that spine BMD, BV/TV and all architectural parameters were significant predictors of multiple vertebral fractures in men. Another investigation based on BMDD and histomorphometry measurements of 25 otherwise healthy males with fragility fractures contrasted with non-fractured historical controls reported a paucity of osteoblasts and osteoclasts on most bone surfaces, a shift to lower mineralization densities for cancellous bone values.[52]

In male rats with osteoporosis induced by orchiectomy (ORX) analyzed by histomorphometry at 2, 4, 8, and 16 weeks post-ORX, bone mineral content (BMC) was reduced at 16 weeks. Trabecular bone volume was significantly decreased from the 4th week.[53] Male rats with osteoporosis caused by spinal cord injury had decreased mineral-to-matrix ratio measured by Raman spectroscopy in both femora and humeri compared to a non-injured control, with no changes in carbonate substitution.[54]

Secondary Osteoporosis

In addition to osteoporosis associated with aging, discussed above, secondary causes can lead to increased fracture risk. This secondary osteoporosis may be induced by glucocorticoids (steroid-induced osteoporosis), thiazide diuretics, opioids, anti-viral therapies and numerous other drugs routinely used in management of non-skeletal conditions[55]. Conditions such as hemophilia[56] and prolonged bed rest can also result in secondary osteoporosis. We have reviewed the changes in bone quality caused by these drugs elsewhere[40]; here we present two examples, the most common form of secondary osteoporosis, that induced by steroids[57] and that associated with treatment for chronic obstructive pulmonary disease (COPD).

Treatment with steroids results in marked increases in fracture incidence without significant changes in bone quantity (BMD) and thus provides an indication of the impact of changes in bone quality. Osteoporotic fractures occur in 30–50% of patients on chronic glucocorticoid therapy.[58] Bones of prednisolone-treated mice had the number of osteocyte lacunae increased; the elastic modulus around the lacunae decreased and an area of hypomineralized bone surrounded the lacunae contrasted with placebo-treated controls.[59] In the treated-mice vertebrae trabecular BV/TV and cortical thickness Ct.Th decreased. Histomorphometry confirmed the decrease in bone volume fraction and showed reduced trabecular thickness, increased trabecular separation and decreased mineral apposition rate along with increased osteocyte apoptosis. There was also reduced bone formation and increased bone resorption. Raman spectroscopy showed a reduced mineral-to-matrix ratio. In a related mouse model of Cushing's syndrome, which produces excessive endogenous steroids and develops osteoporosis, using in situ X-ray nanomechanical imaging, synchrotron micro-computed tomography and scanning electron microscopy investigations, a recent study found that the steroid-enriched animals, as compared to wildtype, lacked a uniform cortex, with their posterior cortex being thinner compared to the anterior.[60] The affected mice cortices had numerous localized cement lines surrounding low mineralized tissue near cavities, in contrast with uniform density in the WT. BMDD data showed the mean calcium content was reduced in endosteal areas, and the tissue heterogeneity was decreased in these areas in the affected mice. WT bone contained a homogeneous network of condensed canals and osteocyte lacunae across the cortical bone while the affected mice had most of these spaces replaced with cavities. Tissue-level stiffness was decreased, maximum strain increased and breaking stress was reduced in bones of the affected mice compared to WT. Collagen fibril deformation was also affected in this model.

Few studies of glucocorticoid-induced osteoporosis in humans include bone quality measurements. In one study[61] men taking glucocorticoids were subdivided into those with

and without vertebral fractures and high resolution CT data combined with finite element methods was used to predict fracture risk; results surpassed those based on BMD. HR-pQCT was also used to characterize changes in bone architecture in women with systemic lupus erythematosus (SLE) treated long-term with glucocorticoids. Cortical thinning and increased cortical porosity were the features of longitudinal microstructural deterioration in treated individuals.[62]

In addition to lupus and rheumatoid arthritis, asthma and other conditions in which glucocorticoids are used for extended periods, fracture risk is increased in individuals with chronic obstructive pulmonary disease (COPD) taking inhaled steroids. While life-style features leading to COPD also affect bone turnover and fracture risk,[63] there is a single study[64] comparing bone quality in newly formed and older bone of individuals with COPD who did and did not sustain fragility fractures based on Raman spectroscopy. Interestingly, no differences were noted between the glucocorticoid-treated individuals with COPD and those who were not treated with glucocorticoids. Those individuals with COPD who had fragility fractures, however, had reduced nanoporosity and elevated mineral-to-matrix ratios and pyridinoline values relative to those without fragility fractures in areas formed two weeks prior to the biopsy. Unfortunately, there are not yet similarly detailed studies on the other agents that cause secondary osteoporosis.

Osteomalacia

Osteomalacia in adults and rickets in children describes conditions in which bones and calcified cartilage are soft (insufficiently mineralized). Generally associated with deficiencies in vitamin D, its metabolites or its receptor, osteomalacia and rickets may also reflect problems with calcium[65] or phosphate[66] handling. Osteomalacia may be diagnosed as osteoporosis because of an increased fracture incidence, but is generally characterized by defective bone mineralization, hypophosphatemia or hypocalcemia. Bone quality in rodents with rickets and osteomalacia was characterized by x-ray diffraction in 1991.[67]

Later, in a small study, we used FTIR microscopy to study human tissues comparing iliac crest biopsies from seven women without apparent bone disease and eleven women diagnosed with osteomalacia.[68] No significant differences in cortical parameters were noted between the two groups of biopsies. The mineral-to-matrix ratio was lower in trabecular regions than in controls. Mineral crystallinity tended to be decreased in osteomalacic trabecular bone, pointing to a sub-optimal mineralization at the bone surface. Another study based on degree of mineralization (BMDD) in 13 individuals reported both lower microhardness and BMDD than controls.[69] Microhardness of the non-mineralized osteoid tissue was 3-fold lower than the total microhardness in the adjacent calcified matrix located in its vicinity. Similarly, histomorphometry of biopsies from adults with hypophosphatasia (due to inactivating mutations in alkaline phosphatase) showed decreased osteoid mineralization and an increased number of osteoblasts, compared both to controls and other individuals with osteomalacia, based on histomorphometry.[70]

X-ray diffraction investigations of mouse models of vitamin D-resistant hypophosphatemic rickets (HYP), showed the bone tissue contained larger crystals in the less mineralized areas at early[67] stages of development; this result was confirmed for older animals by FTIR

microscopy. Pregnant HYP mice were found to have increased porosity by nano-CT.[71] These pregnant HYP mice maintained calcium and vitamin D levels by increasing PTH and activating osteoclasts. Raman analyses of these mice showed increased carbonate-to-phosphate ratio in both the baseline and lactating HYP mouse bones.[72] Bones in another model with increased vitamin D activity, a knockout of the Ca-transporter TRPV5 (transient receptor potential, vanilloid 5) Ca(2+) channel, normally expressed in kidney and osteoclasts, had decreased bone thickness by microCT.[73] These studies are a few examples of osteomalacia and rickets in which bone quality is known to be affected by the improper handling of phosphate and calcium transport. Readers are referred to recent papers on FGFR1, FGF23, PTH, and KLOTHO for more details of other related systems.[74,75]

Osteogenesis Imperfecta

Osteogenesis imperfecta, also known as brittle bone disease, is a group of genetic abnormalities resulting in the inappropriate synthesis, folding, modification and transport of type I collagen, and hence affects all tissues containing this collagen, especially bones and teeth.[76] These mutations cause the bones of individuals with OI to fracture, with typical brittle behavior (Fig. 4), such that after the bone begins to yield, there is minimal post-yield deflection. Bone quality in mouse models of OI has been shown to be abnormal by almost all the methodologies mentioned in this review, including x-ray diffraction,[77] infrared imaging,[78,79, 80,81], BMDD measurements,[82,83] Raman spectroscopy,[84,85,86,87] atomic force microscopy (AFM),[87] second harmonic generation[88] and mechanical testing.[85,89,90] Of interest, most models, and the majority of the human forms of OI are hypermineralized, perhaps, because of the deficiency in type I collagen. Table 2 summarizes bone quality in several well-characterized mouse models studied by one or more of these techniques. Data on bone quality exist for the mild to severe forms of OI but not yet for models of the perinatal lethal form (Type II OI). Bones from humans with OI have been characterized less frequently; limited human data exist for type II OI based on similar analytical methods (Table 3).[94–97] The mouse and human data are in agreement, typically finding hypermineralization, improper mineral alignment with collagen, and altered collagen fibril properties. The brittle behavior appears to be both a function of the abnormal collagen and related changes in the matrix leading to abnormal mineralization patterns.

Osteopetrosis

Failure of bone to be remodeled results in retention of calcified cartilage along with characteristics of older bone, and frequent fractures in the condition known as osteopetrosis. As reviewed elsewhere, osteopetrosis is generally associated with a defect in one or more osteoclastic resorption mechanisms.[98] Similar to most of the conditions mentioned in this review, these abnormalities result in altered bone quality and increased fracture risk. The condition may be caused by genetic abnormalities in regulators of osteoclast activity or by excessive suppression of bone turnover.[99] Bone quality in osteopetrosis was characterized in the toothless rat and the osteopetrotic mouse by x-ray diffraction[100,101] and FTIRI;[101,102] the latter showing microhardness was increased in osteopetrotic bone, the former demonstrated the persistence of small crystals. The c-src knockout mice, which also develop osteopetrosis, had increased numbers of microcracks; however, adult animals with this knockout were not mechanically weaker than control mice when tested in three-point

bending.[103] Bone tissue of another knockout mouse with osteopetrosis, $Fos^{-/-}$, had a more homogeneous matrix based on BMDD due to the persistence of calcified cartilage.[104] Mice with carbonic anhydrase deficiency, also critical for osteoclast-mediated remodeling, provide another model of osteopetrosis. These animals have smaller bones, and the normalized cortical bone volume was similar to that in wildtype bones; however, they had significant metaphyseal widening of the tibial plateau. Trabecular BV/TV was increased almost 50% relative to WT. Histomorphometry showed significant decreases in bone formation rate, and increased number of osteoclasts.[105] In humans, a case report of two non-related male and female individuals with osteopetrosis, HR-pQCT found increased density, increased cortical thickness, high trabecular number and thickness, increased BV/TV. Relative to unaffected controls, the tissue was extremely heterogeneous, with islets of dense bone interposed with areas of normal density.[106] Thus, the fractures in osteopetrotic bone seem to be related to the presence of calcified cartilage, a failure to correct micro-cracks, and, similar to OI, but present for different reasons, smaller crystals.

Conclusions

Age-dependent changes in bone quality in animals and humans and the alterations due to bone diseases have been discussed. As emphasized in this review, rodents are the most commonly-used animals to investigate aging and bone disease. Our ability to manipulate the mouse genome and associated molecular signaling pathways has advanced our understanding of the regulation of bone mass. However, as reviewed elsewhere[107], key differences exist in the rodent skeleton when compared to humans. In particular, rodents lack osteonal remodeling, continue longitudinal bone growth after sexual maturity, and do not undergo a true menopause. Nevertheless, advantages and the similarities in age-related bone loss make rodents a good model to study changes in bone quality.

Alterations in bone quality and tissue mechanical properties at both the micro- and macro-levels have been correlated in a variety of studies, as reviewed recently.[108] Hence understanding how bone quality parameters are modified by both aging and disease should lead to improved treatments to modify bone tissue mechanical properties associated with these conditions, and a reduction in weakened bones and fractures. We have noted how both increases and decreases in the average size of the mineral crystals can lead to fractures; and, how decreased and increased cross-linking of collagen can have similar effects. Changes in micro-architecture and chemical composition of the matrix and mineral are important. Hopefully this review has provided the reader with insight into the importance of understanding these variables and their alterations in some rare and common conditions.

Acknowledgments

Dr. Boskey’s research was supported by NIH grants AR041325 and DE04141.

References

1. Seeman E. Bone quality: the material and structural basis of bone strength. J Bone Miner Metab. 2008; 26:1–8. [PubMed: 18095057]

2. Bouxsein ML. Bone quality: where do we go from here? Osteoporos Int. 2008; 14(Suppl 5):S118–27.

3. Hernandez C, Keaveny TM. A biomechanical perspective on bone quality. Bone. 2006; 39:1173–1181. [PubMed: 16876493]

4. Hunt H, Donnelly EL. Bone quality assessment techniques: geometric, compositional, and mechanical characterization from macroscale to nanoscale. Clin Rev Bone Min Metab. 2016; 14:133–149.

5. Fyhrie DP, Christiansen BA. Bone material properties and skeletal fragility. Calcif Tissue Int. 2015; 97:213–228. [PubMed: 25939648]

6. Engelke K, Libanati C, Fuerst T, et al. Advanced CT based in vivo methods for the assessment of bone density, structure, and strength. Curr Osteoporos Rep. 2013; 11:246–255. [PubMed: 23712690]

7. Campbell GM, Sophocleous A. Quantitative analysis of bone and soft tissue by micro-computed tomography: applications to ex vivo and in vivo studies. Bonekey Rep. 2014; 3:564. [PubMed: 25184037]

8. Compston JE. Histomorphometric interpretation of bone biopsies for the evaluation of osteoporosis treatment. Bonekey Rep. 2012; 1:47. [PubMed: 23951449]

9. Henriksen K, Christiansen C, Karsdal MA. Role of biochemical markers in the management of osteoporosis. Climacteric. 2015; 18(Suppl 2):10–18. [PubMed: 26507704]

10. Bae WC, Patil S, Biswas R, et al. Magnetic resonance imaging assessed cortical porosity is highly correlated with μCT porosity. Bone. 2014; 66:56–61. [PubMed: 24928498]

11. Paschalis EP, Gamsjaeger S, Dempster D, et al. Fragility fracture incidence in chronic obstructive pulmonary disease (COPD) patients associates with nanoporosity, Mineral/Matrix ratio, and Pyridinoline content at actively bone-forming trabecular surfaces. J Bone Miner Res. 2016; doi: 10.1002/jbmr.2933

12. Unal M, Yang S, Akkus O. Molecular spectroscopic identification of the water compartments in bone. Bone. 2014; 67:228–236. [PubMed: 25065717]

13. Schrof S, Varga P, Galvis L, et al. 3D Raman mapping of the collagen fibril orientation in human osteonal lamellae. J Struct Biol. 2014; 187:266–275. [PubMed: 25025981]

14. Unal M, Akkus O. Raman spectral classification of mineral- and collagen-bound water's associations to elastic and post-yield mechanical properties of cortical bone. Bone. 2015; 81:315–26. [PubMed: 26211992]

15. Seref-Ferlengez Z, Kennedy OD, Schaffler MB. Bone microdamage, remodeling and bone fragility: how much damage is too much damage? Bonekey Rep. 2015; 4:644. [PubMed: 25848533]

16. Brock GR, Kim G, Ingraffea AR, et al. Nanoscale examination of microdamage in sheep cortical bone using synchrotron radiation transmission x-ray microscopy. PLoS One. 2013; 8:e57942. [PubMed: 23472121]

17. Turunen MJ, Saarakkala S, Rieppo L, et al. Comparison between infrared and Raman spectroscopic analysis of maturing rabbit cortical bone. Appl Spectrosc. 2011; 65:595–603. [PubMed: 21639980]

18. Gamsjaeger S, Mendelsohn R, Boskey AL, et al. Vibrational spectroscopic imaging for the evaluation of matrix and mineral chemistry. Curr Osteoporos Rep. 2014; 12:454–464. [PubMed: 25240579]

19. Paschalis EP, Mendelsohn R, Boskey AL. Infrared assessment of bone quality: a review. Clin Orthop Relat Res. 2011; 469:2170–2178. [PubMed: 21210314]

20. Morris MD, Mandair GS. Raman assessment of bone quality. Clin Orthop Relat Res. 2011; 469:2160–2169. [PubMed: 21116756]

21. Paschalis EP, Gamsjaeger S, Hassler N, Klaushofer K, Burr D. Ovarian hormone depletion affects cortical bone quality differently on different skeletal envelopes. Bone. 2017; 95:55–64. [PubMed: 27826024]

22. Boskey AL, Donnelly E, Boskey E, et al. Examining the relationships between bone tissue composition, compositional heterogeneity, and fragility fracture: A matched case-controlled FTIRI study. J Bone Miner Res. 2016; 31:1070–1081. [PubMed: 26636271]

23. Tarnowski CP, Ignelzi MA Jr, Morris MD. Mineralization of developing mouse calvaria as revealed by Raman microspectroscopy. J Bone Miner Res. 2002; 17:1118–1126. [PubMed: 12054168]
24. Miller LM, Little W, Schirmer A, et al. Accretion of bone quantity and quality in the developing mouse skeleton. J Bone Miner Res. 2007; 22:1037–1045. [PubMed: 17402847]
25. Raghavan M, Sahar ND, Kohn DH, Morris MD. Age-specific profiles of tissue-level composition and mechanical properties in murine cortical bone. Bone. 2012; 50:942–953. [PubMed: 22285889]
26. Fuchs RK, Allen MR, Ruppel ME, et al. In situ examination of the time-course for secondary mineralization of Haversian bone using synchrotron Fourier transform infrared microspectroscopy. Matrix Biol. 2008; 27:34–41. [PubMed: 17884405]
27. Gourion-Arsiquaud S, Burket JC, Havill LM, et al. Spatial variation in osteonal bone properties relative to tissue and animal age. J Bone Miner Res. 2009; 24:1271–1281. [PubMed: 19210217]
28. Burket J, Gourion-Arsiquaud S, Havill LM, et al. Microstructure and nanomechanical properties in osteons relate to tissue and animal age. J Biomech. 2011; 44:277–284. [PubMed: 21074774]
29. Khosla S. Pathogenesis of age-related bone loss in humans. J Gerontol A Biol Sci Med Sci. 2013; 68:1226–1235. [PubMed: 22923429]
30. Farr JN, Khosla S. Skeletal changes through the lifespan--from growth to senescence. Nat Rev Endocrinol. 2015; 11:513–521. [PubMed: 26032105]
31. Zebaze RM, Ghasem-Zadeh A, Bohte A, et al. Intracortical remodelling and porosity in the distal radius and post-mortem femurs of women: a cross-sectional study. Lancet 2010. 2010; 375:1729–1736.
32. Seeman E. Pathogenesis of bone fragility in women and men. Lancet. 2002; 359:1841–1850. [PubMed: 12044392]
33. Garcia I, Chiodo V, Ma Y, et al. Evidence of altered matrix composition in iliac crest biopsies from patients with idiopathic juvenile osteoporosis. Connect Tissue Res. 2016; 57:28–37. [PubMed: 26539896]
34. Gourion-Arsiquaud S, Faibish D, Myers E, et al. Use of FTIR spectroscopic imaging to identify parameters associated with fragility fracture. J Bone Miner Res. 2009; 24:1565–1571. [PubMed: 19419303]
35. Paschalis EP, Fratzl P, Gamsjaeger S, et al. Aging versus postmenopausal osteoporosis: bone composition and maturation kinetics at actively-forming trabecular Surfaces of Female Subjects Aged 1 to 84 Years. J Bone Miner Res. 2016; 31:347–357. [PubMed: 26308158]
36. Hudelmaier M, Kollstedt A, Lochmüller EM, et al. Gender differences in trabecular bone architecture of the distal radius assessed with magnetic resonance imaging and implications for mechanical competence. Osteoporos Int. 2005; 16:1124–1133. [PubMed: 15744451]
37. Vale AC, Aleixo IP, Lúcio M, et al. At the moment of occurrence of a fragility hip fracture, men have higher mechanical properties values in comparison with women. BMC Musculoskelet Disord. 2013; 14:295. [PubMed: 24131745]
38. Cvijanović O, Lekić A, Nikolić M, et al. Bone quality assessment in individuals of different age, gender and body constitution. Coll Antropol. 2010; 34(Suppl 2):161–168. [PubMed: 21302716]
39. Kazakia GJ, Nirody JA, Bernstein G, et al. Age- and gender-related differences in cortical geometry and microstructure: Improved sensitivity by regional analysis. Bone. 2012; 52:623–631. [PubMed: 23142360]
40. Boskey AL, Imbert L. Effects of drugs on bone quality. Clin Rev Bone Min Metab. 2016; 14:167–196.
41. Roschger P, Paschalis EP, Fratzl P, et al. Bone mineralization density distribution in health and disease. Bone. 2008; 42:456–466. [PubMed: 18096457]
42. Hofstaetter JG, Hofstaetter SG, Nawrot-Wawrzyniak K, et al. Mineralization pattern of vertebral bone material following fragility fracture of the spine. J Orthop Res. 2012; 30:1089–1094. [PubMed: 22228585]
43. Misof BM, Gamsjaeger S, Cohen A, et al. Bone material properties in premenopausal women with idiopathic osteoporosis. J Bone Miner Res. 2012; 27:2551–2561. [PubMed: 22777919]
44. Paschalis EP, Betts F, DiCarlo E, et al. FTIR microspectroscopic analysis of human iliac crest biopsies from untreated osteoporotic bone. Calcif Tissue Int. 1997; 61:487–492. [PubMed: 9383276]

45. McCreadie BR, Morris MD, Chen TC, et al. Bone tissue compositional differences in women with and without osteoporotic fracture. Bone. 2006; 39:1190–1195. [PubMed: 16901772]
46. Kim G, Cole JH, Boskey AL, et al. Reduced tissue-level stiffness and mineralization in osteoporotic cancellous bone. Calcif Tissue Int. 2014; 95:125–131. [PubMed: 24888692]
47. Föger-Samwald U, Vekszler G, Hörz-Schuch E, et al. Molecular mechanisms of osteoporotic hip fractures in elderly women. Exp Gerontol. 2016; 73:49–58. [PubMed: 26608808]
48. Isaksson H, Turunen MJ, Rieppo L, et al. Infrared spectroscopy indicates altered bone turnover and remodeling activity in renal osteodystrophy. J Bone Miner Res. 2010; 25:1360–1366. [PubMed: 20200925]
49. Isaksson H, Töyräs J, Hakulinen M, et al. Structural parameters of normal and osteoporotic human trabecular bone are affected differently by microCT image resolution. Osteoporos Int. 2011; 22:167–177. [PubMed: 20349043]
50. Abraham AC, Agarwalla A, Yadavalli A, et al. Multiscale Predictors of Femoral Neck In Situ Strength in Aging Women: Contributions of BMD, Cortical Porosity, Reference Point Indentation, and Nonenzymatic Glycation. J Bone Miner Res. 2015; 30:2207–2214. [PubMed: 26060094]
51. Legrand E, Chappard D, Pascaretti C, et al. Trabecular bone microarchitecture, bone mineral density, and vertebral fractures in male osteoporosis. J Bone Miner Res. 2000; 15:13–19. [PubMed: 10646109]
52. Fratzl-Zelman N, Roschger P, Misof BM, et al. Fragility fractures in men with idiopathic osteoporosis are associated with undermineralization of the bone matrix without evidence of increased bone turnover. Calcif Tissue Int. 2011; 88:378–387. [PubMed: 21318401]
53. Audran M, Chappard D, Legrand E, et al. Bone microarchitecture and bone fragility in men: DXA and histomorphometry in humans and in the orchidectomized rat model. Calcif Tissue Int. 2001; 69:214–217. [PubMed: 11730253]
54. Shen J, Fan L, Yang J, et al. A longitudinal Raman microspectroscopic study of osteoporosis induced by spinal cord injury. Osteoporos Int. 2010; 21:81–87. [PubMed: 19436936]
55. Mirza F, Canalis E. Management of endocrine disease: Secondary osteoporosis: pathophysiology and management. Eur J Endocrinol. 2015; 173:R131–R151. [PubMed: 25971649]
56. Anagnostis P, Karras S, Paschou SA, et al. Haemophilia A and B as a cause for secondary osteoporosis and increased fracture risk. Blood Coagul Fibrinolysis. 2015; 26:599–603. [PubMed: 26126168]
57. Weinstein RS. Clinical practice. Glucocorticoid-induced bone disease. N Engl J Med. 2011; 365:62–70. [PubMed: 21732837]
58. Mazziotti G, Angeli A, Bilezikian JP, Canalis E, et al. Glucocorticoid-induced osteoporosis: an update. Trends Endocrinol Metab. 2006; 17:144–149. [PubMed: 16678739]
59. Lane NE, Yao W, Balooch M, et al. Glucocorticoid-treated mice have localized changes in trabecular bone material properties and osteocyte lacunar size that are not observed in placebo treated or estrogen-deficient mice. J Bone Miner Res. 2006; 21:466–476. [PubMed: 16491295]
60. Karunaratne A, Xi L, Bentley L, et al. Multiscale alterations in bone matrix quality increased fragility in steroid induced osteoporosis. Bone. 2016; 84:15–24. [PubMed: 26657825]
61. Graeff C, Marin F, Petto H, et al. High resolution quantitative computed tomography-based assessment of trabecular microstructure and strength estimates by finite-element analysis of the spine, but not DXA, reflects vertebral fracture status in men with glucocorticoid-induced osteoporosis. Bone. 2013; 52:568–577. [PubMed: 23149277]
62. Zhu TY, Griffith JF, Qin L, et al. Cortical thinning and progressive cortical porosity in female patients with systemic lupus erythematosus on long-term glucocorticoids: a 2-year case-control study. Osteoporos Int. 2015; 26:1759–1771. [PubMed: 25736166]
63. Okazaki R, Watanabe R, Inoue D. Osteoporosis Associated with Chronic Obstructive Pulmonary Disease. J Bone Metab. 2016; 23:111–120. [PubMed: 27622174]
64. Paschalis EP, Gamsjaeger S, Dempster D, et al. Fragility fracture incidence in chronic obstructive pulmonary disease (COPD) patients associates with nanoporosity, mineral/matrix ratio, and pyridinoline content at actively bone-forming trabecular surfaces. J Bone Miner Res. 2017; 32:165–171. [PubMed: 27490957]

65. Carmeliet G, Dermauw V, Bouillon R. Vitamin D signaling in calcium and bone homeostasis: a delicate balance. Best Pract Res Clin Endocrinol Metab. 2015; 29:621–631. [PubMed: 26303088]
66. Gonciulea AR, Jan De Beur SM. Fibroblast Growth Factor 23-Mediated Bone Disease. Endocrinol Metab Clin North Am. 2017; 46:19–39. [PubMed: 28131132]
67. Boskey AL, Gilder H, Neufeld E, et al. Phospholipid changes inthe bones of the hypophosphatemic mouse. Bone. 1991; 12:345–351. [PubMed: 1782102]
68. Faibish D, Gomes A, Boivin G, et al. Infrared imaging of calcified tissue in bone biopsies from adults with osteomalacia. Bone. 2005; 36:6–12. [PubMed: 15663997]
69. Boivin G, Bala Y, Doublier A, et al. The role of mineralization and organic matrix in the microhardness of bone tissue from controls and osteoporotic patients. Bone. 2008; 43:532–538. [PubMed: 18599391]
70. Barvencik F, Beil FT, Gebauer M, et al. Skeletal mineralization defects in adult hypophosphatasia--a clinical and histological analysis. Osteoporos Int. 2011; 22:2667–2675. [PubMed: 21267545]
71. Boskey A, Frank A, Fujimoto Y, et al. The PHEX transgene corrects mineralization defects in 9-month-old hypophosphatemic mice. Calcif Tissue Int. 2009; 84:126–137. [PubMed: 19082853]
72. Macica CM, King HE, Wang M, et al. Novel anatomic adaptation of cortical bone to meet increased mineral demands of reproduction. Bone. 2016; 85:59–69. [PubMed: 26825813]
73. Nijenhuis T, van der Eerden BC, Hoenderop JG, et al. Bone resorption inhibitor alendronate normalizes the reduced bone thickness of TRPV5(-/-) mice. J Bone Miner Res. 2008; 23:1815–1824. [PubMed: 18597625]
74. Yuan Q, Sato T, Densmore M, et al. FGF-23/Klotho signaling is not essential for the phosphaturic and anabolic functions of PTH. J Bone Miner Res. 2011; 26:2026–2035. [PubMed: 21590742]
75. Han X, Yang J, Li L, et al. Conditional deletion of Fgfr1 in the proximal and distal tubule identifies distinct roles in phosphate and calcium transport. PLoS One. 2016; 11:e0147845. [PubMed: 26839958]
76. Marini JC, Blissett AR. New genes in bone development: what's new in osteogenesis imperfecta. J Clin Endocrinol Metab. 2013; 98:3095–3103. [PubMed: 23771926]
77. Rodriguez-Florez N, Garcia-Tunon E, Mukadam Q, et al. An investigation of the mineral in ductile and brittle cortical mouse bone. J Bone Miner Res. 2015; 30:786–795. [PubMed: 25418329]
78. Coleman RM, Aguilera L, Quinones L, et al. Comparison of bone tissue properties in mouse models with collagenous and non-collagenous genetic L. mutations using FTIRI. Bone. 2012; 51:920–928. [PubMed: 22910579]
79. Boskey AL, Marino J, Spevak L, et al. Are changes in composition in response to treatment of a mouse model of osteogenesis imperfecta sex-dependent? Clin Orthop Relat Res. 2015; 473:2587–2598. [PubMed: 25903941]
80. Masci M, Wang M, Imbert L, et al. Bone mineral properties in growing Col1a2$^{(+/G610C)}$ mice, an animal model of osteogenesis imperfecta. Bone. 2016; 87:120–129. [PubMed: 27083399]
81. Camacho NP, Carroll P, Raggio CL. Fourier transform infrared imaging spectroscopy (FT-IRIS) of mineralization in bisphosphonate-treated oim/oim mice. Calcif Tissue Int. 2003 May; 72(5):604–9. [PubMed: 12574874]
82. Fratzl-Zelman N, Schmidt I, Roschger P, et al. Unique micro- and nano-scale mineralization pattern of human osteogenesis imperfecta type VI bone. Bone. 2015; 73:233–241. [PubMed: 25554599]
83. Fratzl-Zelman N, Morello R, Lee B, et al. CRTAP deficiency leads to abnormally high bone matrix mineralization in a murine model and in children with osteogenesis imperfecta type VII. Bone. 2010; 46:820–826. [PubMed: 19895918]
84. Raghavan M, Sahar ND, Wilson RH, et al. Quantitative polarized Raman spectroscopy in highly turbid bone tissue. J Biomed Opt. 2010; 15:037001. [PubMed: 20615030]
85. Bi X, Grafe I, Ding H, et al. Correlations between bone mechanical properties and bone composition parameters in mouse models of dominant and recessive osteogenesis imperfecta and the response to anti-TGF-β treatment. J Bone Miner Res. 2016; 32:347–359. [PubMed: 27649409]
86. Wallace JM, Orr BG, Marini JC, et al. Nanoscale morphology of Type I collagen is altered in the Brtl mouse model of Osteogenesis Imperfecta. J Struct Biol. 2011; 173:146–152. [PubMed: 20696252]

87. Kozloff KM, Carden A, Bergwitz C, et al. Brittle IV mouse model for osteogenesis imperfecta IV demonstrates postpubertal adaptations to improve whole bone strength. J Bone Miner Res. 2004; 19:614–622. [PubMed: 15005849]

88. Nadiarnykh O, Plotnikov S, Mohler WA, et al. Second harmonic generation imaging microscopy studies of osteogenesis imperfecta. J Biomed Opt. 2007; 12:051805. [PubMed: 17994883]

89. Yao X, Carleton SM, Kettle AD, et al. Gender-dependence of bone structure and properties in adult osteogenesis imperfecta murine model. Ann Biomed Eng. 2013; 41:1139–1149. [PubMed: 23536112]

90. Bart ZR, Hammond MA, Wallace JM. Multi-scale analysis of bone chemistry, morphology and mechanics in the oim model of osteogenesis imperfecta. Connect Tissue Res. 2014; 55(Suppl 1):4–8. [PubMed: 25158170]

91. Saban J, Zussman M, Havey R, Patwardhan A, Schneider G, King D. Heterozygous oim mice exhibit a mild form of osteogenesis imperfecta. Bone. 1996; 19(6):575–579. [PubMed: 8968022]

92. Grabner B, Landis W, Roschger P, et al. Age- and genotype-dependence of bone material properties in the osteogenesis imperfecta murine model (oim). Bone. 2001; 29(5):453–457. [PubMed: 11704498]

93. Bogan R, Riddle RC, Li Z, et al. A mouse model for human osteogenesis imperfecta type VI. J Bone Miner Res. 2013; 28:1531–1536. [PubMed: 23413146]

94. Fratzl-Zelman N, Schmidt I, Roschger P, et al. Mineral particle size in children with osteogenesis imperfecta type I is not increased independently of specific collagen mutations. Bone. 2014; 60:122–128. [PubMed: 24296239]

95. Paschalis EP, Gamsjaeger S, Fratzl-Zelman N, et al. Evidence for a role for nanoporosity and pyridinoline content in human mild osteogenesis imperfecta. J Bone Miner Res. 2016; 31:1050–1059. [PubMed: 26748579]

96. Vetter U, Eanes ED, Kopp JB, et al. Changes in apatite crystal size in bones of patients with osteogenesis imperfecta. Calcif Tissue Int. 1991; 49:248–250. [PubMed: 1760768]

97. Fratzl-Zelman N, Barnes AM, Weis M, et al. Non-Lethal Type VIII Osteogenesis Imperfecta Has Elevated Bone Matrix Mineralization. J Clin Endocrinol Metab. 2016; 101:3516–3525. [PubMed: 27383115]

98. Kocher MS, Kasser JR. Osteopetrosis. Am J Orthop (Belle Mead NJ). 2003; 32:222–228. [PubMed: 12772872]

99. Bargman R, Posham R, Boskey A, et al. High- and low-dose OPG-Fc cause osteopetrosis-like changes in infant mice. Pediatr Res. 2012; 72:495–501. [PubMed: 22926546]

100. Boskey AL, Marks SC Jr. Mineral and matrix alterations in the bones of incisors-absent (ia/ia) osteopetrotic rats. Calcif Tissue Int. 1985; 37:287–292. [PubMed: 3926278]

101. Boskey A. Mineral changes in osteopetrosis. Crit Rev Eukaryot Gene Expr. 2003; 13:109–116. [PubMed: 14696960]

102. Satomura K, Kon M, Tokuyama R, et al. Osteopetrosis complicated by osteomyelitis of the mandible: a case report including characterization of the osteopetrotic bone. Int J Oral Maxillofac Surg. 2007; 36:86–93. [PubMed: 17011167]

103. Nakayama H, Takakuda K, Matsumoto HN, et al. Effects of altered bone remodeling and retention of cement lines on bone quality in osteopetrotic aged c-Src-deficient mice. Calcif Tissue Int. 2010; 86:172–183. [PubMed: 20063091]

104. Roschger P, Matsuo K, Misof BM, et al. Normal mineralization and nanostructure of sclerotic bone in mice overexpressing Fra-1. Bone. 2004; 34:776–782. [PubMed: 15121008]

105. Margolis DS, Szivek JA, Lai LW, et al. Phenotypic characteristics of bone in carbonic anhydrase II-deficient mice. Calcif Tissue Int. 2008; 82:66–76. [PubMed: 18175028]

106. Arruda M, Coelho MC, Moraes AB, et al. Bone mineral density and microarchitecture in patients with autosomal dominant osteopetrosis: A report of two cases. J Bone Miner Res. 2016; 31:657–662. [PubMed: 26387875]

107. Jilka RL. The Relevance of Mouse Models for Investigating Age-Related Bone Loss in Humans. The Journals of Gerontology Series A: Biological Sciences and Medical Sciences. 2013; 68(10): 1209–1217.

108. Bala Y, Seeman E. Bone's material constituents and their contribution to bone strength in health, disease, and treatment. Calcif Tissue Int. 2015; 97:308–326. [PubMed: 25712256]

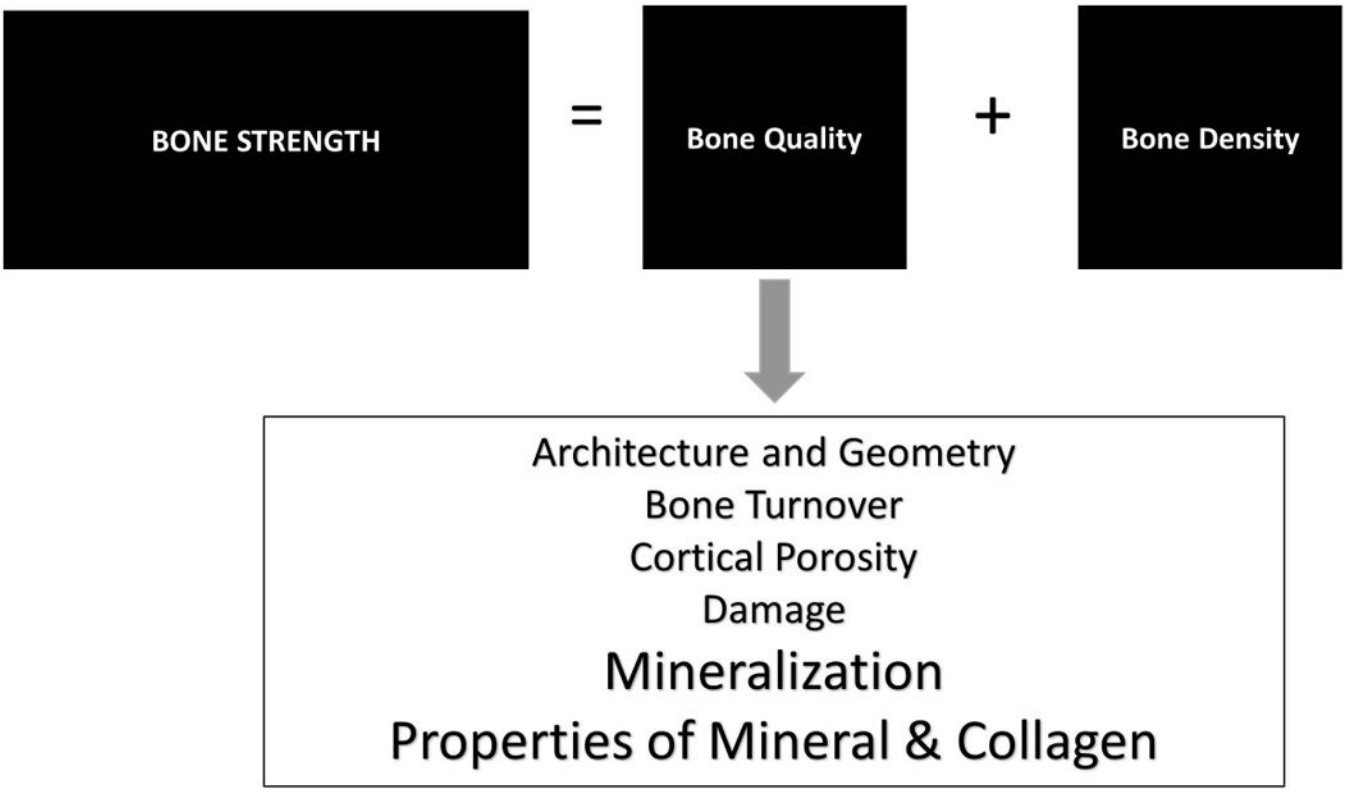

Figure 1.
Schematic illustrating bone quality variables that contribute to fracture risk.

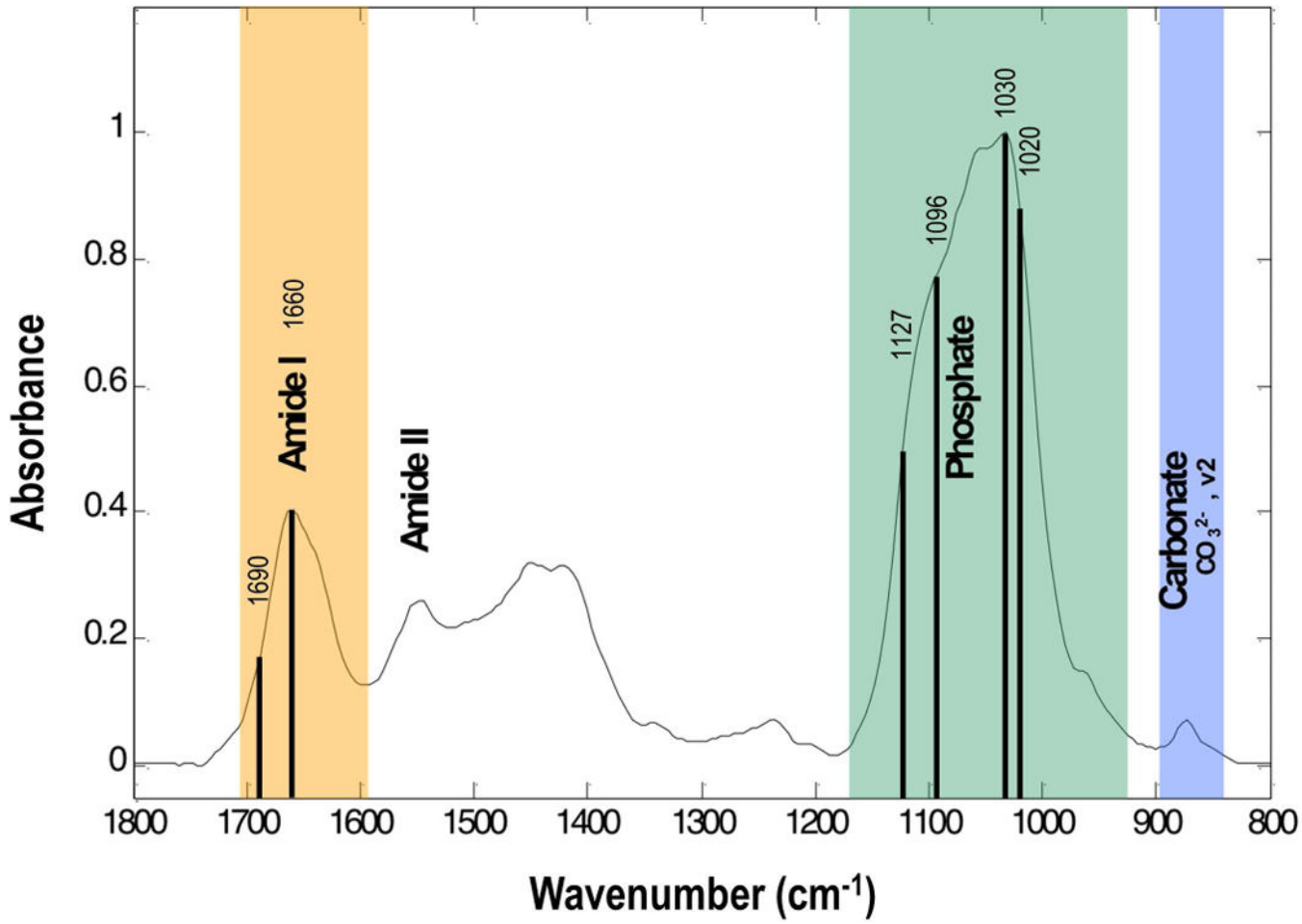

Figure 2.

FTIR spectrum obtained from a single pixel (6.25 × 6.25 μm^2) of an FTIR image. Formulae included for key parameters including mineral/matrix and carbonate/mineral (or carbonate/phosphate) from shaded peak areas and crystallinity, collagen crosslink ratio and acid phosphate substitution from peak height intensities.

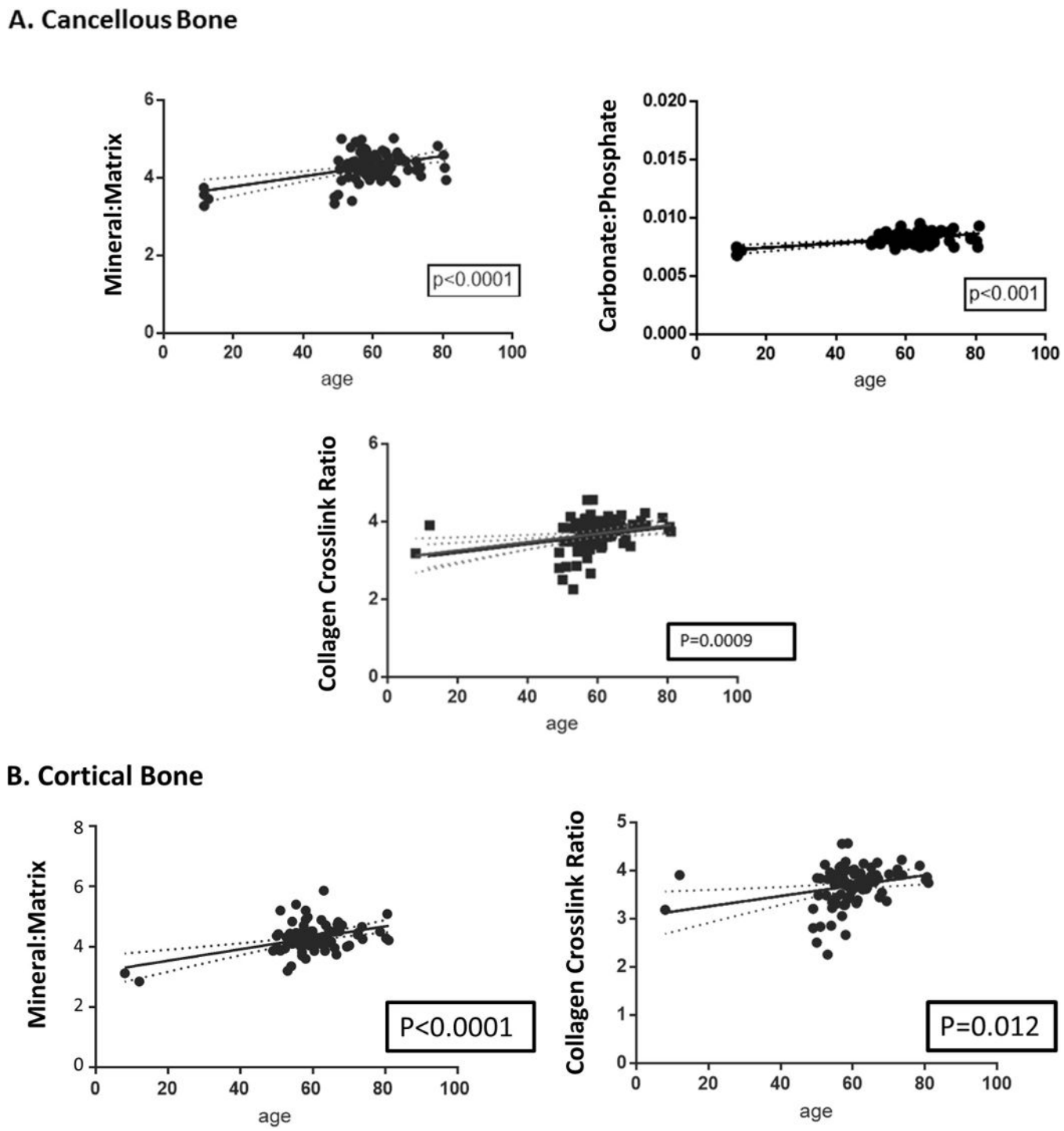

Figure 3.

Correlations between age and FTIRI variable for (A) cortical and (B) cancellous bone were calculated using data for healthy women using GraphPad Prism (version 7.0). Only significant correlations are presented. In some cases, specific parameters, e.g. acid phosphate substitution and carbonate/phosphate, were not measured in all studies due to instrument limitations**.** Solid lines represent best-fit correlations and dotted lines 95% confidence limits.

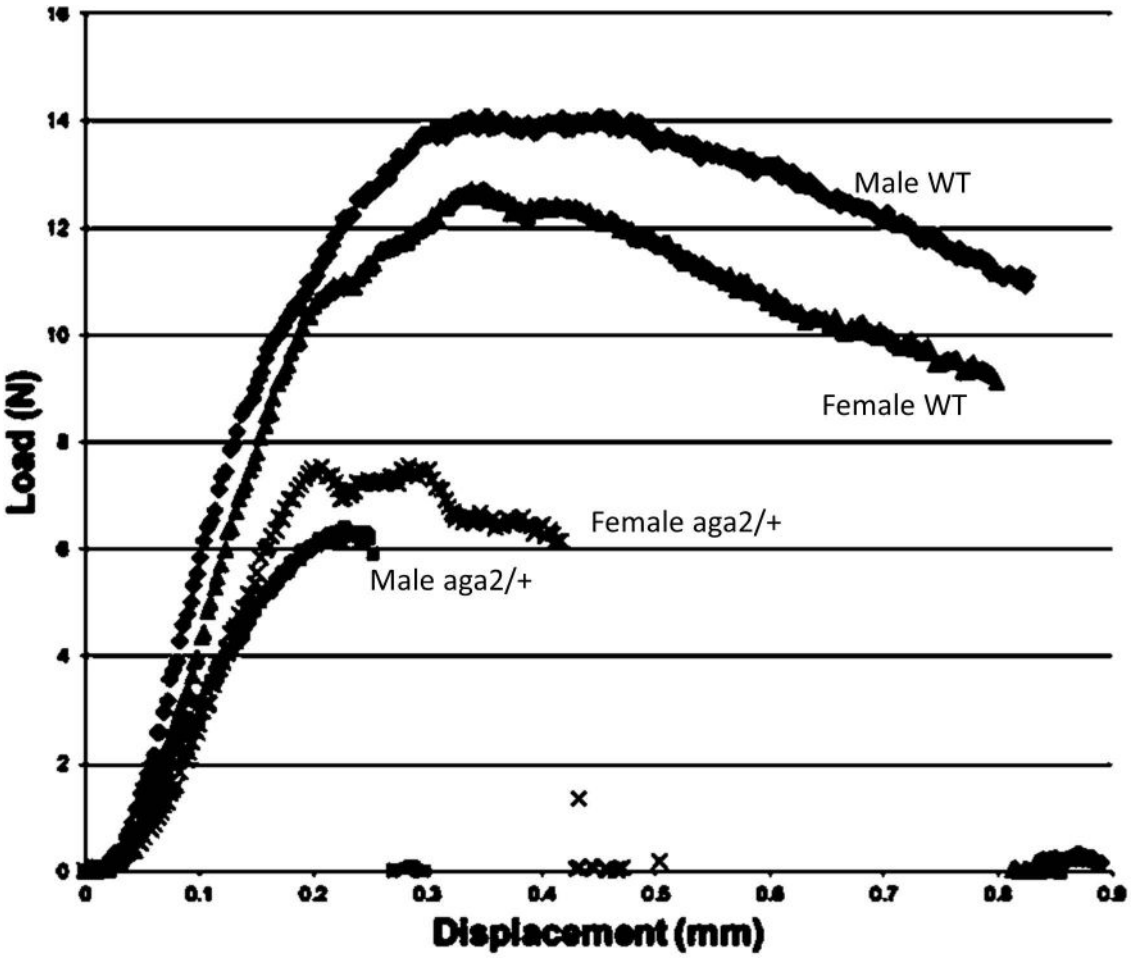

Figure 4.

Typical stress-strain curves from 3-point-bending tests of male and female aga2/+ mice and their wild-type controls. The aga2/+ mice curves end abruptly, showing no post-yield behavior, a characteristic of brittle bone tissue.

Table 1

Spatial Resolution of Techniques used to Characterize Bone Composition and Architecture

Technique	Spatial resolution	Sample preparation	Signal/noise
AFM-IR	20–50 nm	Non-decalcified 300 nm sections	Low
Backscattered electron imaging	0.2 μm	Non-decalcified 100–300 μm sections	High
FT-IR imaging	7–25 μm	Non-decalcified 1–4 μm sections	High
Microcomputed tomography	In vivo < in vitro < high resolution	Minimal	High
NMR	5–10 μm	In vitro and in vivo measurements	Depends on methods used
Raman Imaging	0.5–1 μm	No dehydration needed; limited by specimen chamber	Weak
SEM	10 nm	Thick sections	Noisy
TEM	0.2 nm	Thin sections	
XTEM	1–2 μm	Thin sections	

Table 2

Bone Quality Studies in Mouse Models of Osteogenesis Imperfecta

OI Model	Defect	Techniques Used	Characteristic
Type I +/oim	Autosomal dominant	Mechanical tests[89,91] pCT[89] Raman[89] SAXS[92] Microhardness[92] qBEI[92]	Reduced mechanical properties[91] Sex-dependent composition[89] Reduced hydroxyproline content[89] Increased hardness[92]
Type III *oim/oim* G610C (Amish)	Autosomal dominant; Qualitative-splicing mutation; glycine substitutions	XRD[77] FTIRI[78,79,80,81,90] SHG[88] Raman[84,89] Mechanical tests[90]	Crystals smaller[77,80] Hypermineralized[78,79,80,81] Decreased CO3/PO4[78,79,80] Increased collagen x-links[78,79,80] Crystals not well aligned with collagen[84]; sex-dependent composition[89]; reduced hydroxyproline content[89]; reduced material properties[90] Poorly aligned collagen [81] Decreased Ca content Brittle[90]
Type IV Brtl	Autosomal recessive; Qualitative	Raman[86] microCT[86] AFM[87]	Reduced cortical thickness[86] Less fracture resistant up to 6 mo. of age; mineral/matrix reduced at 6 mo[86]; Collagen d-spacing altered[87]
Type VI *PEDF*$^{-/-}$	Autosomal recessive	Micro-CT, FTIRI, histomorphometry[93] SAXS and BMDD[82]	Reduced trabecular bone volume; accumulation of unmineralized bone; increased mineral/matrix [93] increased Ca content, altered particle alignment with collagen[82]
Fro/fro		FTIRI[78] uCT[78]	Decreased Min/Mat[78]; decreased cross-linking[78]
Type VII *Crtap*$^{-/-}$	Autosomal recessive Defective 3′-OH- prolylase complex	Micro-CT[85,81] Raman [85] Mechanical tests [85] FTIRI[81] Backscattered electron imaging [83]	Hypermineralization; increased mineral/matrix; decreased crystal size; sex-dependent differences in material properties[81]

Table 3

Bone Quality Changes in Human Osteogenesis Imperfecta (OI) Bone Tissue

OI Type	Mutation	Technique	Observation vs. Control
OI Type I	qualitative and quantitative combined type I collagen mutations	qBEI, SAXS, BMDD[90] Raman (newly formed tissue)[91]	No change in particle width; OI tissue denser packing of particles [90] Relative GAG content reduced, nano-porosity reduced, PYD content increased in quantitative group Crystallite length reduced – both[91]
OI Type II	perinatal lethal – type I collagen mutations	X-ray diffraction[92]	Small crystals [92]
OI Type VI	mutation in SERPINF1 leading to loss-of- function of pigment epithelium-derived factor (PEDF)	BMDD, SAXS	Highly mineralized matrix with low mineral content [93]
OI Type VII	hypomorphic mutations with CRTAP expression	BMDD	Increased mineralization[81]
OI Type VIII	null mutations in P3H1, encoding prolyl 3- hydroxylase 1.	Histomorphometry, qBEI, BMDD	Decreased cortical width; thin trabeculae; patches of increased osteoid; hypermineralization [94]